International Journal of Technology 14(1) 152-161 (2023)
Received August 2021 / Revised September 2021 / Accepted October 2021

International Journal of Technology

Nanofiber Cellulose/Lignin from Oil Palm Empty Fruit Bunches and the Potential for Carbon Fiber Precursor Prepared by Wet-spinning

Mahyuni Harahap[1,2], Nurkholidah Daulay[3], Devi Zebua[3], Saharman Gea[2,3*]

[1]*Department of Chemistry, Faculty of Science Technology and Information, Universitas Sari Mutiara Indonesia, Jalan Kapten Muslim, Medan 20124, Indonesia*
[2]*Cellulosic and Functional Materials Research Centre, Universitas Sumatera Utara, Jalan Bioteknologi No.1, Medan 20155, Indonesia*
[3]*Department of Chemistry, Faculty of Mathematics and Natural Science, Universitas Sumatera Utara, Jalan Bioteknologi No.1, Medan 201555, Indonesia*

Abstract. This work isolated nanofiber cellulose (NFC) and Lignin from oil palm empty fruit bunches (OPEFB). NFC/lignin-based carbon fiber was prepared by using the wet-spinning technique and followed by pyrolysis at 500°C. Lignin isolated from OPEFB was compared with commercial Lignin by using Fourier Transform Infrared (FTIR). The nano dimension of NFC was observed by using Transmission Electron Microscope (TEM). The NFC/lignin after pyrolysis was characterized by using SEM EDX and Raman spectroscopy. NFC showed diameters between 5 nm and 60 nm. Both Lignin commercial and isolated had aromatic benzene. Lignin was introduced to NFC, where NFC/lignin composition of (100:0), (90:10), and (80:20) increased the thermal stability of wet-spun fiber. Meanwhile, NFC/lignin (90:10) and (80:20) had almost 50% residual mass. The result confirmed that the carbon material, such as NFC/lignin (100:0), (90:10), and (80:20), had rod-like shape morphology with diameters of 236.2 nm, 492.4 nm, and 653.2 nm, respectively. Furthermore, the G band and D band of the carbonous material were observed at 1580 cm^{-1} and 1358 cm^{-1}. The conversion of NFC/lignin from OPEFB to carbon material was successful and potentially suitable for the precursor of carbon fiber.

Keywords: Carbon fiber; Lignin; Nanofiber cellulose; Oil palm empty fruit bunches

1. Introduction

Carbon fiber is a great research interest because of its large surface area, high porosity, low density, sufficient electrical conductivity, and lightweight. Carbon fiber demand was reported to increase by 10% annually (Wang *et al.,* 2019), as it has become an important engineering material due to its unique and attractive mechanical properties (stronger than steel and aluminum). Carbon fiber reinforces polymer-matrix composites in advanced materials.

Polyacrylonitrile (PAN) is the most suitable precursor for carbon-based material, accounting for high-performance carbon fiber, high melting point, and rich carbon content. However, PAN is petroleum-based with complex and costly manufacturing processes of the functional materials, whose cost could be twice the carbon processing cost (Baker and Rials,

*Corresponding author's email: s.gea@usu.ac.id, Tel.: 085297978578, Fax.: (061) 8214290
doi: 10.14716/ijtech.v14i1.5082

2013). Furthermore, the increase in environmental awareness has sparked an interest in materials produced from natural resources. Therefore, green carbon source as an alternative to replacing petroleum-based polymers is more favored in manufacturing carbon fiber.

Cellulose, the most abundant biomass resource, originated from plants and microorganisms such as algae and tunicate. The utilization of cellulose reduced the dependence on fossil resources and protected the environment. Cellulose is environmentally friendly, abundantly available, renewable, biodegradable, and biocompatible. However, the use of cellulose as the precursor for carbon fiber has some limitations, such as relatively low carbon content and aromatic absence in the biopolymers. Nanofiber cellulose (NFC), highly crystalline cellulose, has been used to improve the properties of material cellulose-based, *i.e.,* nanofiber composite (Misran *et al.,* 2020), printed electronics (Hoeng, Denneulin, and Bras, 2016), biomedicine (Lin and Dufresne, 2014), nanocomposite (Helmiyati and Anggraini, 2019), nanofiltration membrane (Rochardjo *et al.,* 2021), and filler for carbon fiber (Harahap *et al.* 2019).

Lignin, the second most abundant biomass in the world, is a major potential source of renewable aromatic resources (Ház *et al.,* 2019). It consists of three main phenylpropane units, such as guaiacol (G), sryingyl (S), and p-hydroxyphenyl (H), at different proportions depending on the sources and extraction process. In the pulp industry, only 1%-2% of Lignin produced could be utilized, while the rest was usually discharged directly to the sewage which could cause serious environmental pollution (Baker and Rials, 2013). A review of "global lignin supply overview and kraft lignin potential as an alternative to petroleum-based polymer" stated that kraft lignin production increased by 150% between 2014 and 2018, and market pull for Lignin is projected between 2023 and 2028. Lignin has been a proven alternative to petroleum energy, mainly due to its availability at around one-third of the solid matter in woods (Dessbesell *et al.,* 2020). Preparing a high-value lignin-based material remains a prominent issue in order to utilize this natural biopolymer fully and reduce the contamination from pulp industry, considering low mechanical properties of Lignin where tensile modulus, strength, and strain-to-failure-values-were-accounted-for 52 ± 2 GPa, 1.04 ± 0.10 GPa, and 2.0 ± 0.2%, respectively (Zhang and Amod, 2014).

Several studies have reported the potential of lignin application in advanced materials by combining Lignin with other polymers or modifying it. Lignin-polyvinyl alcohol nanofiber was formulated for microelectrode applications (Roman *et al.,* 2019). Other literature converted lignin-polyacrylonitrile to carbon nanofiber (Ma, Li,, and Chang, 2015). Lignin was also acetylated to enhance its functionality and exploit its application areas (Zhao *et al.,* 2017). Wang *et al.* (2019) isolated nanocellulose from pulp hardwood and spun it with commercial Lignin to produce conductive carbon microfibers. In addition, Geng *et al.* (2021) produced a highly strong and conductive carbon fiber based-nanocellulose from jute fiber and sodium lignosulfonate crosslinked by chitosan molecule.

In this study, we aim to prepare biodegradable and green carbon fiber by using NFC and Lignin from oil palm empty fruit bunches (OPEFB). Our previous study reported a simple method to extract NFC and Lignin from OPEFB without producing by-product (Gea *et al.,* 2020). To the best of our knowledge, there is no study yet reported carbon fiber-based NFC and Lignin derived from OPEFB. We expect that blending NFC and Lignin would increase the mechanical properties of lignin-based carbon fiber. Furthermore, the production cost of NFC/lignin-based carbon fiber is estimated to be lower than petroleum-based carbon fiber.

2. Methods

OPEFB was obtained from PTPN IV Adolina, North Sumatra, Indonesia. The materials used in this experimental were HNO_3, $NaNO_2$, NaOH pellets (≥98%), $NaSO_3$, NaOCl (2.5%), H_2O_2 (30%), HCl (37%), H_2SO_4 (98%), DMSO (98%) purchased from Merck (Darmstadt, Germany). All materials were used without further purification.

2.1. Isolation of Nanofiber Cellulose and Lignin from Oil Palm Empty Fruit Bunches

OPEFB was cut into small pieces with lengths around 1 cm. They were dried in a vacuum oven at 100°C for six h. Next, 75 g of dried OPEFB was put into a three-necked flask where 1 L HNO_3 3.5% and 10 mg $NaNO_2$ were added. The mixture was refluxed for two h at 90°C. The residue was collected and washed with deionized water several times until pH was close to 7. After that, 375 mL NaOH 2% and 375 mL $NaSO_3$ 2% were added, and the reflux was continued for one h at 50°C. Next, the residue was collected and washed with deionized water until pH 7, while the filtrate was collected for the lignin isolation process.

The washed residue was bleached by using 250 mL NaOCl 1.75% for 30 minutes at 70°C, followed by washing with deionized water several times until pH close to 7 and the addition of 500 mL NaOH 17.5% at 80°C for 30 minutes. After that, it was further purified by using 250 mL H_2O_2 10% at 60°C for 30 minutes. The sample was dried in the vacuum oven at 60°C for five h. NFC was extracted using 10% HCl ultrasonication (Ultrasonic Processor UP 100H, Hielscher Ultrasonic Technology, Denmark) for three h. The solution was allowed to cool at room temperature for 24 h before the residue was collected at the bottom of the flask. The residue was washed using deionized water in vacuum filtration several times. Finally, the product was dried in the vacuum oven at 50°C for five h and coded as NFC.

Next, the filtrate collected for lignin isolation was boiled at 100°C for one h. It was then acidified with 5 N H_2SO_4 5 N until the pH was 2. Next, it was washed with distilled water and centrifuged for 5 min at 8000 rpm at room temperature. Then, it was washed by using deionized water until pH was 7. The Lignin was dried in the vacuum oven at 50°C for five h. The scheme illustration for NFC and lignin isolation is shown in Figure 1.

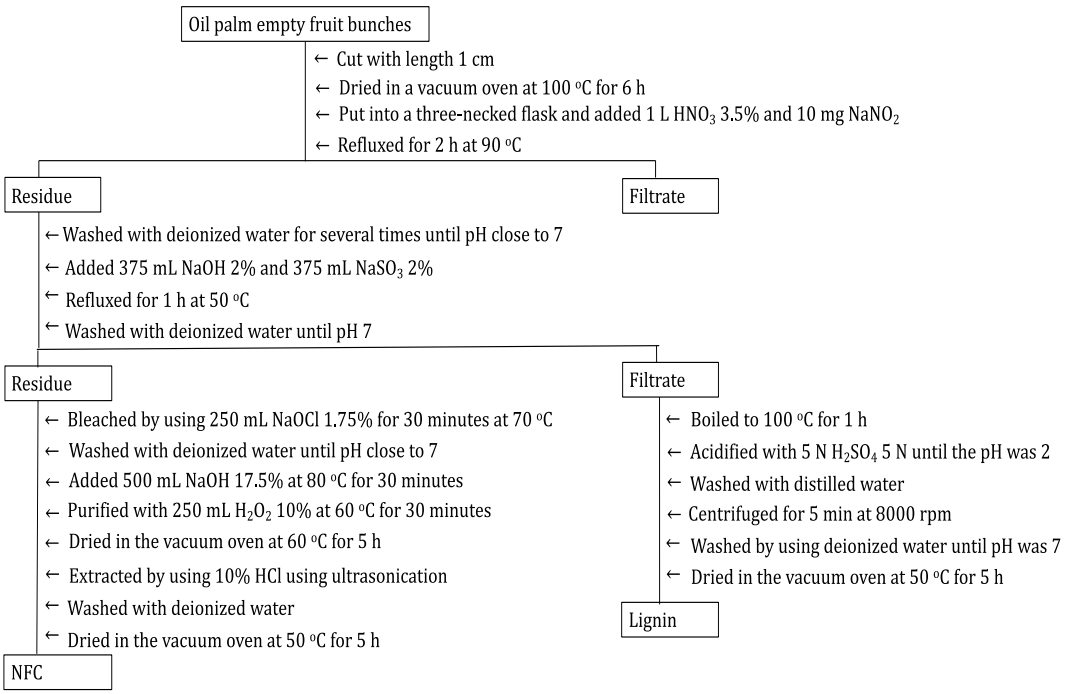

Figure 1 A scheme illustration for NFC and lignin isolation from OPEFB

2.2. Wet-spinning of Nanofiber

NFC was dissolved in DMSO under reflux conditions at 60°C for 12 h with a 10% (w/v) concentration. The solution was allowed to cool at room temperature. The same condition was also carried out for the lignin solution. After that, three polymer solutions (NFC/lignin) with the concentration of (100:0); (90:10); and (80:20) were dispersed by sonication at 24 kHz, 20°C –30°C for 10 minutes. The solutions were spun in a coagulation bath that contained a deionized water solution. The wet-spun condition was as follows: needle diameter of 0.25 mm, feed rate of 0.004 g/minute, and wind speed of 0.44 m/minute. The spun fiber was dried at room temperature and coded as NFC/lignin (100:0); NFC/lignin (90:10); and NFC/lignin (80:20).

2.3. Carbonization of Wet-spun Fiber

Carbonization of the wet-spun NFC/lignin fibers was performed by using a tube furnace under a nitrogen atmosphere (200 mL/minute). First, 3 g of the sample was placed in a graphite sample holder and placed inside the tube furnace. Then, pyrolysis with a heating rate of 5°C /minute was done in two steps: pre-carbonization from 25°C to 100°C, held isothermally for 30 minutes at 100°C, and carbonization between 100°C and 500°C, held isothermally for 30 minutes at 500°C.

2.4. Characterization

First, the NFC dimension was investigated using JEOL/EO JEM-1400 (Tokyo, Japan) transmission electron microscope operated at an accelerating voltage of 100 kV. A highly diluted NFC solution in distilled water was prepared. The solution was dropped on carbon-coated electron microscope grids and stained with uranyl acetate. Next, the morphology of Lignin and NFC/lignin fiber was characterized by using Hitachi TM3030 (JEOL, Ltd., Tokyo, Japan) scanning electron microscope (SEM). The sample was first coated with a thin layer of gold to reduce charges during analysis. The instrument was operated at an accelerating voltage of 10 kV. Third, the solution's chemical compounds were studied using a Fourier-transform infrared (FTIR) spectrometer (Nicolet 380, Thermo Scientific, Boston, USA), which used a transmission mode with a resolution of 4 cm^{-1} and 100 scans. Fourth, the crystallinity of NFC, Lignin, and NFC/lignin fibers was investigated by using Bruker D8 advanced X-ray diffractometer (Bruker Optik GmbH, Ettlingen, Germany). The instrument was operated at 35 kV and 25 mA. Next, the samples' thermal analysis was carried out using thermogravimetric analysis (TGA) and DTA/TG Exstar SII 7300 (Hitachi medical system, Tokyo, Japan), where 10 mg sample was placed in a platinum pan and tightly closed. The sample was analyzed between 30°C and 600°C at a heating rate of 10°C/min. Finally, the morphology of the carbonized NFC/lignin was observed by using SEM EDX, while the structure was investigated by using Raman spectroscopy (Raman microscope enclosure, RE-04, Renishaw, UK) using a 785 nm laser. The samples were analyzed without any treatment. The analyzed region was visualized through a microscope with 50x magnification. The range of wavelengths collected was typically from 150 to 3200 cm^{-1} over a time period of at least 30 seconds and multiple accumulations for high sensitivity.

3. Results and Discussion

3.1. FTIR Analysis

FTIR spectra for NFC and Lignin isolated from OPEFB, commercial Lignin, wet-spun NFC/lignin are shown in Figure 2. Both isolated and commercial Lignin had OH groups stretching in phenolic and aliphatic structures at wavenumber 3430 cm^{-1}. C-H stretching in methyl and methylene groups and methoxy groups was shown at the absorption bands of 2925 cm^{-1} and 2850 cm^{-1}, respectively. Two string vibrations were observed at 1515 cm^{-1}

and 1637 cm^{-1} corresponding to the aromatic benzene ring. Syringyl units in Lignin were seen at 1328 cm^{-1}, 1228 cm^{-1}, and 1125 cm^{-1} bands, whereas guaiacyl structures appeared at 1272 cm^{-1} and 1032 cm^{-1} bands (Arun *et al.*, 2020). The band at 1168 cm^{-1} corresponded to the carbonyl stretching of conjugated ester groups. Similarly, the band from 1000 cm^{-1} to 800 cm^{-1} attributed to C-O, C-H, and C=O aromatic out-of-the-plane deformation in Lignin (Arun *et al.*, 2020).

NFC/lignin spun-fiber showed absorption bands between 4000 and 3200 cm^{-1} corresponding to the hydroxyl groups (-OH) of water. This trend has become larger compared to isolated and commercial Lignin. In addition, C-O of the alcohol group in NFC could be clearly seen in NFC/lignin spun-fiber at the 1087 cm^{-1} to 1026 cm^{-1} band. For NFC, O-H and H-C-H stretching (alkyl, aliphatic) were seen at 3278 cm^{-1} and 2890 cm^{-1}, respectively. The band at 1640 cm^{-1} corresponded to fiber-OH (absorbed water), 1429 cm^{-1} attributed to HCH and OCH bending vibrations (methylene group), and 1371 cm^{-1} referred to CH deformation vibration (CH_3 or OH in plane). The band confirmed COC, CCO, and CCH deformation and stretching vibrations at 896-915 cm^{-1} (Xie *et al.*, 2016).

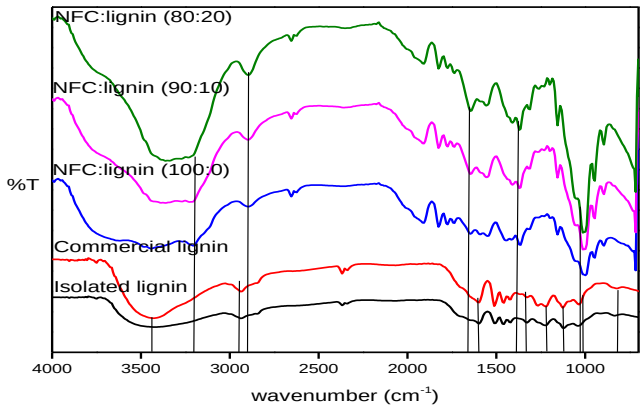

Figure 2 FTIR spectra of NFC, isolated Lignin, commercial Lignin, NFC/lignin (100:0), NFC/lignin (90:10), and NFC/lignin (80:20)

3.2. Morphological Analysis

The dimension of NFC was analyzed using TEM, while the morphological analysis of Lignin and wet-spun NFC/lignin was carried out using SEM. TEM micrograph of NFC and SEM images of Lignin and wet-spun NFC/lignin are shown in Figures 3 and 4, respectively.

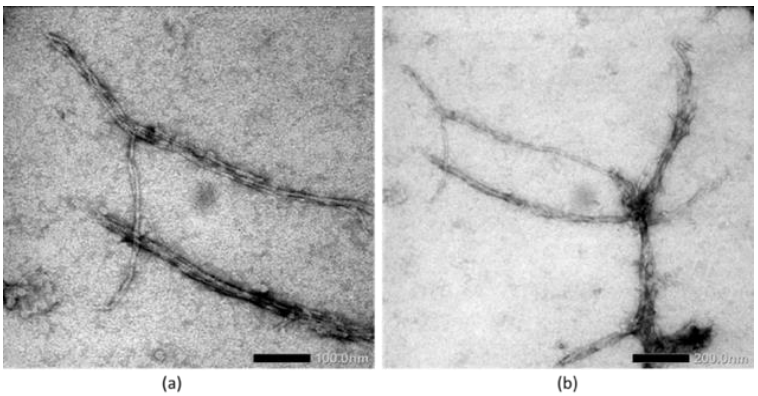

Figure 3 TEM micrograph of NFC isolated from OPEFB with (a) 100 nm and (b) 200 nm scale bars

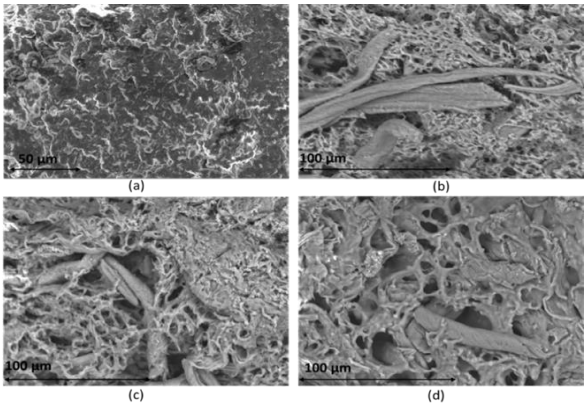

Figure 4 SEM micrographs of: (a) lignin, (b) NFC/lignin (100:0), (c) NFC/lignin (90:10), and (d) NFC/lignin (80:20) with 1.0 K magnification

With reference to Figure 2, NFC showed long fibers and web-like shapes with diameters between 5 nm and 60 nm. The same result was reported by another study claiming that NFC from pineapple peels isolated by the steam explosion had a diameter in size range of 5–60 nm (Cherian *et al.,* 2010). On the other hand, the dimension of NFC isolated from Ushar (*Calotropid Procea*) was in size range of 10–20 nm (Oun and Rhim, 2016), whereas the NFC from cotton linter was in the size of 12 nm (Morais *et al.,* 2013). The shape and dimension of NFC were commonly affected by the source of cellulose, isolation method, and reaction condition.

The SEM images of Lignin isolated from OPEFB (Figure 3.a) had a uniform, flake-like, rough surface morphology. However, SEM images of NFC/lignin 100:0, 90:10, and 80:20 (Figure 3.b, 3.c, and 3.d) showed non-uniform morphology. They looked like single fibers but attached to each other. Pores were observed on those fibers, where the higher the lignin content, the bigger the pore sizes were. NFC/lignin (80:20) showed particles on the fiber surface that were not observed in NFC/lignin (100:0) and (90:10). This appearance may be due to the sonication time of NFC/lignin that was being too short. Higher lignin content should be sonicated longer with more lignin particles dispersed into NFC.

3.3. Thermogravimetric Analysis

The thermal stability of Lignin, NFC, and NFC/lignin (90:10, and 80:20) was analyzed using thermogravimetric analysis (TGA). The TGA traces for all samples are presented in Figure 5. All samples had a three-stage processing time function indicating sample weight loss.

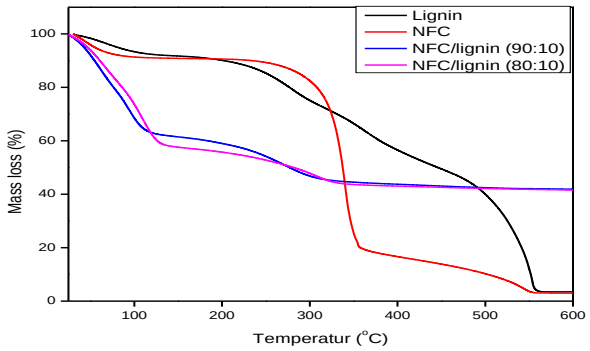

Figure 5 TGA curve for Lignin, NFC, NFC/lignin (100:0), NFC/lignin (90:10), and NFC/lignin (80:20)

The first step for pure Lignin and NFC was from 25°C to 120 °C where water content was removed. The second step was between 280°C and 380°C for NFC, whereas

230°C –580°C for Lignin. The two biopolymers almost lost all their mass at 600°C. Next, NFC/lignin (100:0) spun-fiber had the most prominent trend at the first step at 25°C to 150°C, where the remaining residual mass was approximately 20%. At 600°C, there was only a tiny percent of residual mass loss. Wet-spun NFC/lignin (90:10) showed a similar TGA curve to NFC/lignin (80:20). The first step occurred from 25°C to 120°C with around 20% mass loss. The second step was between 120°C and 320°C with a residual mass around 50%. At the last step, no mass loss occurred. Blending lignin and NFC could improve the material thermal stability. Previous literature reported that TG curves for composite lignin/NFC had three major weight losses starting from 50-100°C corresponding to the elimination of absorbed water, at 200-400°C was for polymer decomposition and chain scission of Lignin and NFC. Above 400°C was for carbonization. The presence of Lignin up to 75 wt% increased the residual mass up to 45.78% (Geng *et al.*, 2021).

3.4. XRD Analysis

XRD analysis was carried out to confirm the crystallinity of NFC before and after blending with Lignin. Figure 6 shows the XRD pattern for Lignin, NFC, and wet-spun NFC/lignin (90:10). Lignin had an 18.30°-18.40° reflection attributed to the amorphous phase. At the same time, NFC had 22.3° reflection assigned to the crystallinity of NFC. This peak was high owing to NFC being a high crystalline material, with crystallinity >70% (Gea *et al.*, 2020). From the pattern, NFC had the structure of cellulose I with two theta reflection at 14.5° – 15.3°, 15.7°–16.30°, and 21.90°–22.20° attributed to (1-10), (100), and (200) crystallographic plane respectively. The presence of Lignin in the NFC did not disturb the crystallinity.

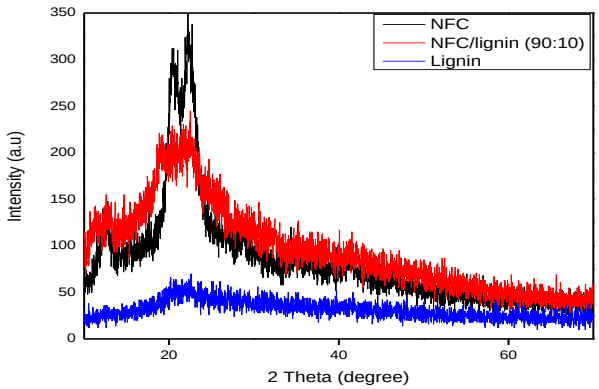

Figure 6 XRD pattern of lignin, NFC, and NFC/lignin (90:10)

3.5. Characterization of Carbon Fibers

3.5.1. SEM EDX Analysis

The morphology of wet-spun NFC/lignin after carbonization was investigated by using SEM EDX, as shown in Figure 7. Carbon fiber from NFC/lignin (100:0) Figure 7(a) shows the rod-like shape morphology. This sample had the smoothest surface morphology compared to the other fibers. The morphology of NFC/lignin (90:10) Figure 7(b) also shows a rod-like shape, but the fibers were stacked at each other. On the other hand, NFC/lignin (80:20) Figure 7(c) had rod-like and spherical morphology. The diameters were directly measured by using an SEM EDX machine, providing 236.2 nm, 492.4 nm, and 653.2 nm measurements for carbon fiber NFC/lignin (100:0), (90:10), and (80:20), respectively. All samples had approximately 50% oxygen and >25% sodium and carbon content. NFC/lignin (90:10) and NFC/lignin (80:20) contained 0.06% sulfur and 0.05% silicon. Another study reported that carbon fiber derived from Lignin and NFC pyrolyzed at 1000°C had >80%

carbon content (Geng *et al.*, 2020). Higher temperatures would increase the carbon content and decrease the oxygen content.

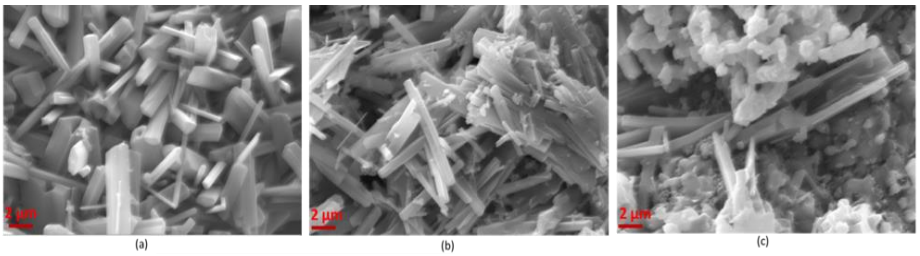

Figure 7 SEM images of wet-spun NFC/lignin (100:0), NFC/lignin (90:10), and NFC/lignin (80:20) carbon fibers

3.5.2. Raman Analysis

Raman spectroscopy studied the carbon structure of wet-spun NFC/lignin (100:0; 90:10; and 80:20). The Raman spectra for the carbon fiber are presented in Figure 8. The crystalline structure of carbon material in Raman spectroscopy showed four spectral regions to indicate either amorphous or the crystalline parts in carbon as summarized in the following: D (1350-1370 cm^{-1}), G (1575-1582 cm^{-1}), D' (~1620 cm^{-1}) and G' (2690-2730 cm^{-1}). G-band was for sp^2 bonding of C=C bonds in the graphitic structures with E_{2g} vibration mode. It is normally presented in a single graphite crystal. Whereas, D-band represented sp^3 bonding in poorly graphitized fibers. Therefore, according to the Tuinstra-Koenig equation, the ID/IG ratio could determine the order level of carbon materials. The peak at ~1620 cm^{-1} appeared for non-graphitized fibers; whereas the band at 2690-2730 cm^{-1} presented graphitized fibers (Le *et al.* 2020).

From Figure 7, the peaks for G band and D band were at 1580 cm^{-1} and 1358 cm^{-1}, indicating the presence of carbon material in the wet-spun fiber NFC/lignin (100:0; 90:10; and 80:20) with I_D/I_G values of 0.84, 0.86, and 0.84 respectively. The results provided information that the carbonization process for all wet-spun fiber was successful, and the fiber had a potential use for carbon fiber precursor. However, in the next study, the pyrolysis temperature could be increased to 1000°C in order to obtain higher G band. Table 1 summarises several applications of carbon fiber derived from biomass.

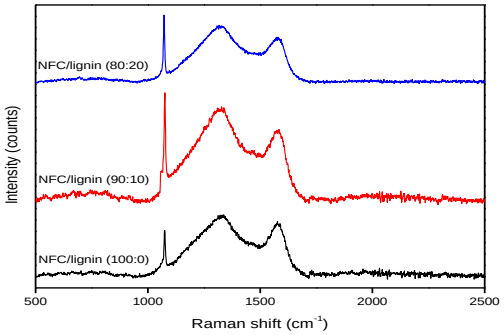

Figure 8 Raman spectra of NFC/lignin (100:0), NFC/lignin (90:10), and NFC/lignin (80:20) carbon fibers

Table 1 Carbon fiber derived from biomass

Raw material	Method	Application	References
Bamboo	Lay-up method	Composite	(Pramono, Rebet, and Zulfa, 2017)
Nanocellulose from jute fibre/sodium lignosulfonate	Wet-spinning	Conductive carbon fibre	(Geng *et al.*, 2021)
Nanocellulose/lignin	Wet-spinning	Conductive carbon fibre	(Wang *et al.*, 2019)

4. Conclusions

NFC-isolated OPEFB have diameters between 5 nm and 60 nm with long fibers and web-like shapes, whereas Lignin has uniform, flake-like, and rough surface morphology. The introduction of Lignin into NFC nanofiber increases the thermal stability and residual mass and maintains the crystallinity. Carbon fiber from wet-spun NFC/lignin carbonized at 500°C has rod-like shape morphology. NFC/lignin (100:0) has the smoothest surface morphology compared to other carbon fibers. The diameter of the carbon fiber increases with the presence of Lignin into NFC, where diameters of 236.2 nm, 492.4 nm, to 653.2 nm have resulted in NFC/lignin (100:0), (90:10), (80:20) samples respectively. The carbon content of all samples is >25%. Raman spectroscopy confirms the G band (1580 cm^{-1}) and D band (1358 cm^{-1}) for all carbonous NFC/lignin indicating the presence of carbon material in the samples. The carbonization process for all wet-spun NFC/lignin fiber is successful, and the fiber can be used as a carbon fiber precursor.

Acknowledgments

This research received no specific grant from any funding agencies in the public, commercial, or not-for-profit sectors.

References

Arun, V., Perumal, E.M., Prakash, K.A., Rajesh, M., Tamilarasan, K., 2020. Sequential fractionation and characterization of lignin and cellulose fiber from waste rice bran. *Journal of Environmental Chemical Engineering,* Volume 8(5), pp. 1–19

Baker, D.A., Rials, T.G., 2013. Recent advances in low-cost carbon fiber manufacture from lignin. *Journal of Applied Polymer Science,* Voulme 130(2), pp. 713–28

Cherian, B.M., Leao, A.L., Souza, S.F.d., Thomas, S., Pothan, L.A., Kottaisamy, M., 2010. Isolation of nanocellulose from pineapple leaf fibres by steam explosion. *Carbohydrate Polymers*, Volume 81(3), pp. 720–25

Dessbesell, L., Paleologou, M., Leitch, M., Pulkki, R., Xu, C.C., 2020. Global lignin supply overview and kraft lignin potential as an alternative for petroleum-based polymers. *Renewable and Sustainable Energy Reviews,* Volumer 123, pp. 109768

Gea, S., Siregar, A.H., Zaidar, E., Harahap, M., Indrawan, D.P., Perangin-angin, Y.A., 2020. Isolation and characterisation of cellulose nanofibre and lignin from oil palm empty fruit bunches. *Materials,* Volume 13(10), pp. 2290

Geng, L., Cai, Y., Lu, L., Zhang, Y., Li, Y., Chen, B., Peng, X., 2021. Highly strong and conductive carbon fibers originated from bioinspired lignin/nanocellulose precursor obtained by flow-assited alignmnet and in situ interfacial complexation. *ACS Sustainable Chemistry & Engineering.* Volume 9(6), pp. 2591–2599

Geng, S., Wei, J., Jonasson, S., Hedlund, J., Oksman, K., 2020. Multifunctional carbon aerogels with hierarchical anisotropic structure derived from lignin and cellulose nanofibers for CO_2 capture and energy storage. *ACS Applied Materials and Interfaces,* Volume 12(6), pp. 7432–41

Harahap, M., Hararak, B., Khan, I., Pandita, S., Gea, S., 2019. Wet-spinning of cellulose acetate reinforced with acetylated nano-crystalline cellulose as carbon fibre precursors. *IOP Conference Series: Materials Science and Engineering,* Volumee 553, pp. 1–8

Ház, A., Jablonsky, M., Surina, I., Kacik, F., Bubenikova, T., Durkovic, J., 2019. Chemical composition and thermal behavior of kraft lignins. *Forests,* Volume 10(6), pp. 1–12

Helmiyati, Anggraini, Y., 2019. Nanocomposites comprising cellulose and nanomagnetite as heterogeneous catalysts for the synthesis of biodiesel from oleic acid. *International Journal of Technology,* Volume 10(4), pp. 808–17

Hoeng, F., Denneulin, A., Bras, J., 2016. Use of nanocellulose in printed electronics: a review. *Nanoscale,* Volume 8(27), pp. 13131–54

Le, N.D., Trogen, M., Ma, Y., Varley, R.J., Hummel, M., Byrne, N., 2020. Cellulose-lignin composite fibers as precursors for carbon fibers: part 2–the impact of precursor properties on carbon fibers. *Carbohydrate Polymers,* Volume 250, pp. 116918

Lin, N., Dufresne, A., 2014. Nanocellulose in biomedicine: current status and future prospect. *European Polymer Journal,* Volume 59, pp. 302–25

Ma, A., Li. Z., Chang, J, 2015. Conversion of lignin-nanofibers to CNFs. *Nano,* Volume 10(6), pp. 1–9

Misran, E., Wirdjosentono, B., Noor, N.M., Gea, S., Situmorang, S.A., Harahap, M., 2020. Preparation and characterisation of electrospun composite nanofibre polyvinyl alcohol/nanofibrillated cellulose isolated from oil palm empty fruit bunches. *BioResources,* Volume 15(4), pp. 7906–17

Morais, J.P.S., Rosa, M.d.F., Filho, M.M.S., Nascimento, L.D., Nascimento, D.M., Cassales, A.R., 2013. Extraction and characterization of nanocellulose structures from raw cotton linter. *Carbohydrate Polymers,* Volume 91(1), pp. 229–35

Oun, A.A., Rhim, J.W., 2016. Characterization of nanocelluloses isolated from ushar (*calotropis procera*) seed fiber: effect of isolation method. *Materials Letters,* Volume 168, pp. 146–50

Pramono, A.E., Rebet, I., Zulfa, A., 2017. Electrical and mechanical properties of phenolic resin and gigantochloa apus carbon fibre composite. *International Journal of Technology*, Volume 5, pp. 920–929

Rochardjo, H.S.B., Fatkhurrohman., Ahmad, K., Yudhanto, F., 2021. Fabrication of nanofiltration membrane based on polyvinyl alcohol nanofibers reinforced with cellulose nanocrystal using electrospinning techniques. *International Journal of Technology,* Volume 12(2), pp. 329

Roman, J., Neri, W., Derré, A., Poulin, P., 2019. Electrospun lignin-based twisted carbon nanofibers for potential microelectrodes applications. *Carbon,* Volume 145, pp. 556–64

Wang, L., Ago, M., Borghei, M., Ishaq, A., Papageorgiou, A.C.P., Lundahl, M., Rojas, O.J., 2019. Conductive carbon microfibers derived from wet-spun lignin/nanocellulose hydrogels. *ACS Sustainable Chemistry and Engineering,* Volume 7(6), pp. 6013–22

Xia, Z., Li, J., Zhang, J., Zhang, X., Zheng, X., Zhang, J., 2020. Processing and valorization of cellulose, lignin and lignocellulose using ionic liquids. *Journal of Bioresources and Bioproducts,* Volume 5, pp. 79–98

Xie, J., Hse, C.H., Hoop, C.F.C., Hu, T., Qi, J., Shupe, T.F., 2016. Isolation and characterization of cellulose nanofibers from bamboo using microwave liquefaction combined with chemical treatment and ultrasonication. *Carbohydrate Polymers,* Volume 151, pp. 725–34

Zhang, M., Amod A.O., 2014. Carbon fibers from dry-spinning of acetylated softwood kraft lignin. *Carbon,* Volume 69, pp. 626–29

Zhao, X., Huang, Z., Zhang, Y., Yang, M., Chen, D., Huang, K., Hu, H., Huang, A., Qin, X., Feng, Z., 2017. Efficient solid-phase synthesis of acetylated lignin and a comparison of the properties of different modified lignins. *Journal of Applied Polymer Science*, Volume 134(1), pp. 1–13